International Journal of Neural Systems, Vol. 28, No. 6 (2018) 1750057 (24 pages)

DOI: 10.1142/S0129065717500575

Characterizing EEG Cortical Dynamics and Connectivity with Responses to Single Pulse Electrical Stimulation (SPES)

Gonzalo Alarcón
Comprehensive Epilepsy Center Neuroscience Institute
Academic Health Systems, Hamad Medical Corporation, Doha, Qatar
Department of Clinical Neuroscience, King's College London
Institute of Psychiatry, Psychology and Neuroscience London, UK
Department of Clinical Neurophysiology
King's College Hospital NHS FT, London, UK
Weill Cornell Medical College, Doha, Qatar

Diego Jiménez-Jiménez
Universidad San Francisco de Quito
School of Medicine, Quito, Ecuador
Department of Clinical Neurophysiology
King's College Hospital NHS FT, London, UK
Department of Clinical Neuroscience, King's College London
Institute of Psychiatry, Psychology and Neuroscience London, UK

Antonio Valentín
Department of Clinical Neuroscience
King's College London, Institute of Psychiatry
Psychology and Neuroscience London, UK
Department of Clinical Neurophysiology
King's College Hospital NHS FT, London, UK
Weill Cornell Medical College, Doha, Qatar

David Martín-López
Department of Clinical Neurophysiology
Kingston Hospital NHS FT, London, UK
Department of Clinical Neurophysiology
St George's University Hospitals NHS FT, London, UK
Department of Clinical Neuroscience, King's College London
Institute of Psychiatry, Psychology and Neuroscience London, UK
Weill Cornell Medical College, Doha, Qatar
david.martin_lopez@kcl.ac.uk

Accepted 12 November 2017
Published Online 29 January 2018

Objectives: To model cortical connections in order to characterize their oscillatory behavior and role in the generation of spontaneous electroencephalogram (EEG). Methods: We studied averaged responses to single pulse electrical stimulation (SPES) from the non-epileptogenic hemisphere of five patients assessed with intracranial EEG who became seizure free after contralateral temporal lobectomy. Second-order

control system equations were modified to characterize the systems generating a given response. SPES responses were modeled as responses to a unit step input. EEG power spectrum was calculated on the 20 s preceding SPES. Results: 121 channels showed responses to 32 stimulation sites. A single system could model the response in 41.3% and two systems were required in 58.7%. Peaks in the frequency response of the models tended to occur within the frequency range of most activity on the spontaneous EEG. Discrepancies were noted between activity predicted by models and activity recorded in the spontaneous EEG. These discrepancies could be explained by the existence of alpha rhythm or interictal epileptiform discharges. Conclusions: Cortical interactions shown by SPES can be described as control systems which can predict cortical oscillatory behavior. The method is unique as it describes connectivity as well as dynamic interactions.

Keywords: Forced coupling; single pulse electrical stimulation; control systems; EEG.

1. Introduction

The dynamics of the oscillatory behavior of neuronal systems is largely unknown. Traditional approaches to study electroencephalographic (EEG) brain connectivity and dynamics rely on identifying regions which are driving spontaneous cortical activity. When EEG activity propagates with preserved morphology, as in the case of epileptiform discharges, latency analysis identifying time differences between peaks can characterize propagation patterns and conduction times.[1–3] However, EEG waveforms can change with propagation because activity from different regions may add up and mutually interact. When waveforms are different between recording sites, the phase spectrum of Fourier analysis, spectral coherence and cross correlation have been used to identify leading regions and propagation patterns. Such methods suffer from relatively poor time resolution. Moreover, since Fourier analysis can only be defined for oscillatory (periodic) activity, when phase differences are recorded between two sites, it may be difficult or arbitrary to define which site is leading. A number of nonlinear signal processing methods have been developed over the last decades to overcome some limitations (for review, see Ref. 4). These include nonlinear regression analysis, amount of mutual information and chaos theory. Graph theory is emerging as a method for describing the global and local properties of brain networks (for review, see Ref. 5). Each method is based on specific physiological and statistical assumptions. At present such assumptions tend to be largely theoretical, as it is unclear how multiple regions interact to generate electrical activity in the functioning human brain.

Because a region receives on-going functional contributions from many other brain areas simultaneously, it is difficult to tease out the relative contributions from all regions connected to a particular site. In addition, functional connections are typically reciprocal[6] and each region responds, modifying and feeding back activity from and to all other connected regions within milliseconds. In this process of mutual and multiple modulation of oscillatory activity by many regions, it is difficult to estimate the amount of coupling existing between any two regions.

The intracranial implantation of electrodes in patients being assessed for surgery to treat their epilepsy provides a unique opportunity to study human brain. In the present work, we propose a new approach to estimate functional coupling between two regions and its contribution to spontaneous EEG activity, based on the response of neuronal networks to localized external stimulation. We have previously used responses to single pulse electrical stimulation (SPES) directly applied to the human cortex for interictal identification of hyperexcitable networks responsible to seizures.[7–10] Slight variations of this technique, sometimes denominated cortico-cortical evoked responses (CCEP), have been employed by other groups.[11–20] In addition, responses to SPES have increasingly been studied to map functional cortical connectivity.[6,11,12,14,16–18,21–24]

The pathophysiology of EEG responses to SPES is complex. Early and delayed EEG responses to SPES have been described. Early responses start immediately after stimulus, are seen when stimulating at most sites and can be largely considered as the normal response to stimulation.[7] Delayed responses tend to occur at the seizure onset site,

and can be considered as a biomarker for epileptogenicity in children and adults.[7–9,25] The morphology of early responses tends to be very consistent at each site but can vary largely among regions.[7,16] Early responses often contain an early surface negative deflection (N1) at 22–36 ms and a second negative deflection (N2) usually at 113–164 ms,[11,12,21,26] sometimes showing a wider latency range from 7–127 ms.[15] However, the morphology of early responses can vary between regions, and N1 or N2 deflections may not be present. Early responses have also been described as an initial positive triphasic waveform (within 9.2 ms and 23.8 ms) or an initial negative biphasic waveform (within 25.4 ms and 39.4 ms).[17] In later work, the authors classified response waveforms into three types[22]: (a) Type N–P, the most common type, consisting of an initial negative peak (N1) followed by a positive peak (P1); (b) Type N, consisting of N1 without P1; and (c) Type P, consisting of P1 only.

Cortical responses to electrical stimulation show enormous morphological variability and frequently fail to fit into any of the above descriptions.[7,16] Nevertheless, the overarching morphology of early responses appears to be that of several cycles of oscillations, sometimes resembling the damped sinusoids that describe the response of linear control systems to a step function input.[27] We suggest that single pulse stimuli can be interpreted as a transient function applied to the neuronal network, and waveforms of the EEG responses may reflect the transient steady-state response of the system (the cortex) until baseline level is reached. Excitatory and inhibitory postsynaptic potentials are related to the different response deflections in the anaesthetised cat.[28] The amplitude of early responses behaves broadly linearly over a range of amplitudes: the amplitude of early responses to SPES tend to increase with increasing stimulation intensity and with proximity to stimulating electrodes up to a ceiling,[15,29] suggesting that response amplitude is linearly related to stimulation intensity and that linear models could be appropriate to describe such responses. The amplitude of the response is broadly proportional to the strength of the connection and to the distance from stimulation.

One advantage of linear control theory is that it provides an estimate for the system's response to any frequency, regardless of the frequency composition of a particular input signal. In this sense, the application of control theory would provide an estimate of the ability (likelihood) of connections to generate each possible frequency, and therefore an estimate of the frequencies with which each connection is more likely to contribute to the spontaneous EEG. This is fundamental to the understanding of oscillatory systems such as those generating electrical cortical activity.

Our model assumes the following postulates with regard to cortical responses to SPES:

(1) Presence of a cortical response to stimulation indicates the presence of a functional connection between the stimulated area and the area where a response is recorded.
(2) A single electrical pulse applied to the cortex behaves as a transient input function.
(3) The EEG response reflects the output of the cortical network activated by the connection between stimulated and recorded areas.[27]

The aim of this work is to test the following hypotheses:

(a) Linear control models can be used to describe the morphology of early responses to SPES.
(b) The frequency response of the connections activated by SPES can explain some of the oscillatory behavior of the spontaneous EEG.

If these hypotheses are correct, SPES responses could be used to estimate functional coupling between two regions (stimulated and recorded) and determine the relative contribution of the stimulated region to oscillatory mechanisms in the recorded region. This implies that SPES can be used to identify cortical connections in addition to describing their dynamics, a unique feature not present in any other method to date. In essence, the frequency response of the systems involved can be characterized as Bode plots which describe the system gain at each frequency. Thus, the peak of the Bode plot determines the frequency at which input gain is highest, and therefore the frequency at which the system is most likely to oscillate (the resonant frequency). In addition, the methodology described here can provide a uniform model to describe all response deflexions recorded with a small number of parameters sufficient to characterize oscillations, thus avoiding the use of multiple labels for latencies and amplitudes of peaks which are not always present.

Table 1. Patient information.

Patient	Etiology	Age (years)	Age at seizure onset	Medication	Surgery performed
1	Mesial temporal sclerosis	24	11 months	Carbamazepine, lamotrigine	Right temporal lobectomy
2	Stroke	34	24 years	Oxcarbazepine	Right temporal lobectomy
3	Mesial temporal sclerosis	39	7 years	Levetericetam, clobazam	Right temporal lobectomy
4	Mesial temporal sclerosis	40	13 years	Phenytoin, levetericetam, tegretol	Left temporal lobectomy
5	Mesial temporal sclerosis	32	15 years	Levetericetam, pregabalin, zopiclone	Left temporal lobectomy

2. Methods

2.1. *Subjects*

The study included five patients (Table 1) assessed for surgery with chronic intracranial EEG recordings for the treatment of their epilepsy at King's College Hospital (London) between February 2007 and June 2009 who fulfilled the following inclusion criteria:

(a) Patients had subdural or depth (intracerebral) electrodes bilaterally implanted in the temporal lobes.
(b) Responses to SPES were recorded during assessment.
(c) Patients underwent temporal lobectomy for the treatment of their epilepsy.
(d) Patients became seizure free after surgery.

In order to estimate the behavior of non-epileptic brain, only recordings from the non-epileptic temporal lobes were selected for analysis. Since all selected patients were seizure free after surgery, it is assumed that the remaining temporal lobe was not epileptogenic during the preoperative recordings used. Intracranial recordings cannot be compared with normal controls because it is impossible and unethical for normal subjects to undergo intracranial recordings. At present, the only clinical indication for chronic intracranial recordings is presurgical assessment of epilepsy which is the case of our patients. Therefore, the closest to normal control is the non-epileptogenic hemisphere in patients who become seizure-free after resective surgery, which was the rationale for patient selection in our study. Furthermore, for the study of the mechanisms of the spontaneous EEG, each patient behaves as his/her own control since we compare the compound Bode plot and the spontaneous EEG generated in the same region.

The surgical procedure consisted on en-bloc temporal lobectomies which followed an anatomically standardized surgical technique.[30] En bloc temporal lobectomy was undertaken at King's College Hospital as originally described by Falconer,[31] later modified to achieve a more complete removal of the hippocampus by use of the principles described by Spencer.[32] In effect, between 5.5 cm and 6.5 cm of the temporal lobe was removed. In the dominant hemisphere (the left) all superior temporal gyrus except the anterior 2 cm was spared. Such a resection would have included at least 50% of the amygdala and 2–3 cm of parahippocampal gyrus and hippocampus. The procedure removes most of the temporal lobe with its connections. Therefore, post-surgical seizure freedom after resection will be considered as the gold standard to demonstrate that the focus (including cortical pathology and associated epileptogenic connections) has been removed. Abolition of seizures after surgery suggests that the remaining cortex and connections are not epileptogenic. Some cortex previously connected to the removed focus will remain, which appears unable to generate seizures by itself. The choice of the hemisphere contralateral to the resection for analysis further minimizes the effect of the connections to and from the resected focus.

2.2. *Electrodes*

In accordance to the inclusion criteria above, all patients had bilateral subdural or depth electrodes implanted for intracranial EEG recordings during pre-surgical assessment. Subdural strip electrodes consisted of single rows of 4–8 platinum disk electrodes spaced at 10 mm between centers. The disks were embedded in a 0.7 mm thick polyurethane strip which overlapped the edges, leaving a diameter of 2.3 mm exposed, recessing approximately 0.1 mm from the surface plane. Multicontact flexible bundles

of depth electrodes (AdTech Medical Instruments Corp., WI, USA) were implanted stereotactically under MRI guidance at temporal lobe locations. Each depth electrode bundle contained 6–10 cylindrical 2.3 mm platinum electrodes, with adjacent electrode centers separated by 5 mm. The location of electrodes was verified by post-implantation skull X-ray, brain computed tomography (CT) or magnetic resonance imaging (MRI). The type, number and location of the electrodes were determined by the suspected location of the ictal onset region, according to non-invasive evaluation: clinical history, scalp EEG recordings obtained with the Maudsley system,[33,34] neuropsychology[35] and neuroimaging. The selection criteria and implantation procedure have been described elsewhere.[36]

2.3. *Recording protocol*

The number of electrodes implanted is necessarily limited and was dictated by clinical practice. Recording of intracranial EEG started when the patient had recovered from the general anaesthesia applied for electrode implantation, at least 24 h after the surgery for electrode implantation. Cable telemetry with up to 64 recording channels was used for data acquisition with simultaneous video monitoring. In all five patients, a Medelec-Profile system was used (Medelec, Oxford Instruments, United Kingdom). Data were digitized at 256 Hz and band pass filtered (0.05–70 Hz). The input range was 10 mV and data were digitized with a 22-bit analog-to-digital converter (an amplitude resolution of 0.153 nV). Interictal awake and sleep recordings in addition to ictal recordings and responses to SPES were permanently stored in hard drives. Data were recorded as common reference to a scalp electrode applied half way between Cz and Pz, and displayed for review in a variety of montages.

2.4. *Interictal spontaneous EEG activity*

EEG selected for power spectrum: 20 s of spontaneous EEG recorded immediately prior to starting the SPES protocol were used as a sample of spontaneous EEG in order to estimate the frequency composition of spontaneous EEG activity between 0 Hz and 50 Hz employing the periodogram method. EEG traces contained only periods of wakefulness with eyes open.

Interictal epileptiform discharges: The non-epileptogenic hemisphere often shows independent epileptiform discharges.[1,34] Therefore, interictal telemetry recordings from all patients were inspected in order to identify the presence of interictal discharges in the non-epileptogenic hemisphere. If present, 25 of such interictal discharges were identified and averaged. When more than one type of epileptiform discharges (location or morphology) was observed, each type was averaged independently.

2.5. *SPES protocol*

SPES is used routinely in our center to study cortical excitability and aid in the identification of epileptogenic cortex.[7,8,25] SPES was applied sequentially between pairs of adjacent electrodes with a constant current neurostimulator (Medelec ST10 Sensor, Oxford Instruments or Leadpoint, Medtronic) using monophasic single pulses (0.1 or 0.2 Hz, 1 ms, 5 mA). At least 10 identical stimuli were delivered at each stimulated site with each polarity. All pairs of consecutive electrodes were used to stimulate on successive trials. Monophasic pulses were chosen in order to increase spatial resolution because the cathode is more effective in exciting neurons. We applied 10 pulses with one polarity followed by another 10 pulses with reversed polarity, so that all electrodes were used as cathode at some point. These stimulation parameters are safe (for more details, see Valentin *et al.* 2002[7]) and charge delivered per second is 100 times lower than that applied for routine functional mapping. We have safely used this technique in over 200 patients assessed with intracranial electrodes for pre-surgical assessment of epilepsy. Essentially, 5 mA appears to provide the best compromise between safety and likelihood to record abnormal (delayed) responses while avoiding amplifier clipping as much as possible. EEG responses to each pulse were recorded by the non-stimulating electrodes. For each pair of stimulating electrodes and for each polarity, responses were stored and averaged for analysis.

A more detailed description of the experimental protocol for SPES is described elsewhere.[7–9,25]

2.6. *Mathematical models*

The mathematical development for open and closed second-order linear control models can be found in the Appendix section.

2.7. *Measurement and modeling of responses*

Software was designed and implemented in MatLab R2014a (The Math Works Inc., USA). Responses to identical SPES stimuli were averaged. Responses to stimuli of different polarities were averaged and analyzed separately. Channels obscured by stimulus artifact or containing significant amount of noise were rejected from analysis. Channels that saturated (clipped) were excluded from analysis.

Intracranial responses to SPES were averaged by selecting 4 s epochs centered at the SPES artifact. The time point when the largest amplitude of the stimulation artifact was reached was set as the reference time point for averaging (time zero). Epochs comprising the first 1500 ms after stimulus were used for modeling. Modeling was carried out in the recording montage (common reference to a scalp electrode located half way between Cz and Pz).

Averaged responses to SPES were assumed to contain the unit step response of one or two control systems, each similar to those shown in Fig. 1 but differing in R and/or T. Response parameters (R and T) were measured by fixing manual cursors to the first two peaks of similar polarity in the first cycle of the response. T was defined as the time difference between both peaks. When only one deflection was present, the two peaks of opposite polarity were used and T was defined as twice the time difference between them. R was defined as the attenuation ratio between amplitudes of the first and second peaks (measured from peak to baseline, see Fig. 1), that is, the amplitude attenuation between the first deflection and the second deflection. An example of response modeling is shown in Fig. 2.

As shown by the equations in the Appendix, T and R define ω_n, ω_d and ζ, which are the parameters that determine the output response, $y(t)$. For the values of T and R, the model's response was calculated for the first 1500 ms after stimulus. The first positive or negative deflections distinguishable from the stimulus artifact were used to model the ***first control system***. Frequently, the first deflection was followed by others of similar frequency of oscillation. In these cases, T and R values were identified as described above (Fig. 2) and the response predicted by the corresponding control system was calculated. Once the response predicted by the first control model was calculated, it was subtracted from the original recorded response [Fig. 2(b)]. If a remaining response distinguishable from the background noise was observed in the difference, the same modeling process was reiterated with the difference in order to obtain T and R for the ***second control system*** [Fig. 2(c)]. The interactions stopped if no oscillatory response distinguishable from the background noise was observed in the remaining signal. This was achieved with either one or two control systems

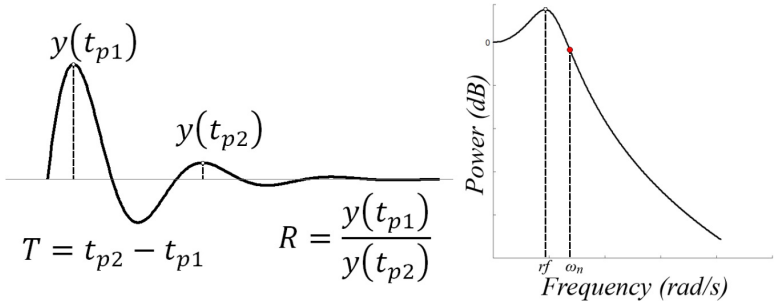

Fig. 1. Representation of a damped oscillation showing the meaning of T (period) and R (subsidence ratio). The natural frequency of the oscillation (the inverse of T) corresponds to $2\pi/\omega_d$. ω_d is the angular frequency of the damped oscillation and equals $\omega_n\sqrt{(1-\zeta^2)}$. The envelope of the response is defined by two curves: $y(t) = 1 + e^{-\zeta\omega_n t}$, and $y(t) = 1 - e^{-\zeta\omega_n t}$. The graph on the right represents the Bode diagram (frequency response) corresponding to a control system of the parameters shown on the left graph. The system gain decreases with frequency for frequencies above the cutoff frequency (ω_n). The system gain is largest at a frequency (resonance frequency, rtf) to the left of the cutoff frequency. The resonance frequency represents the frequency at which the system is most likely to oscillate.

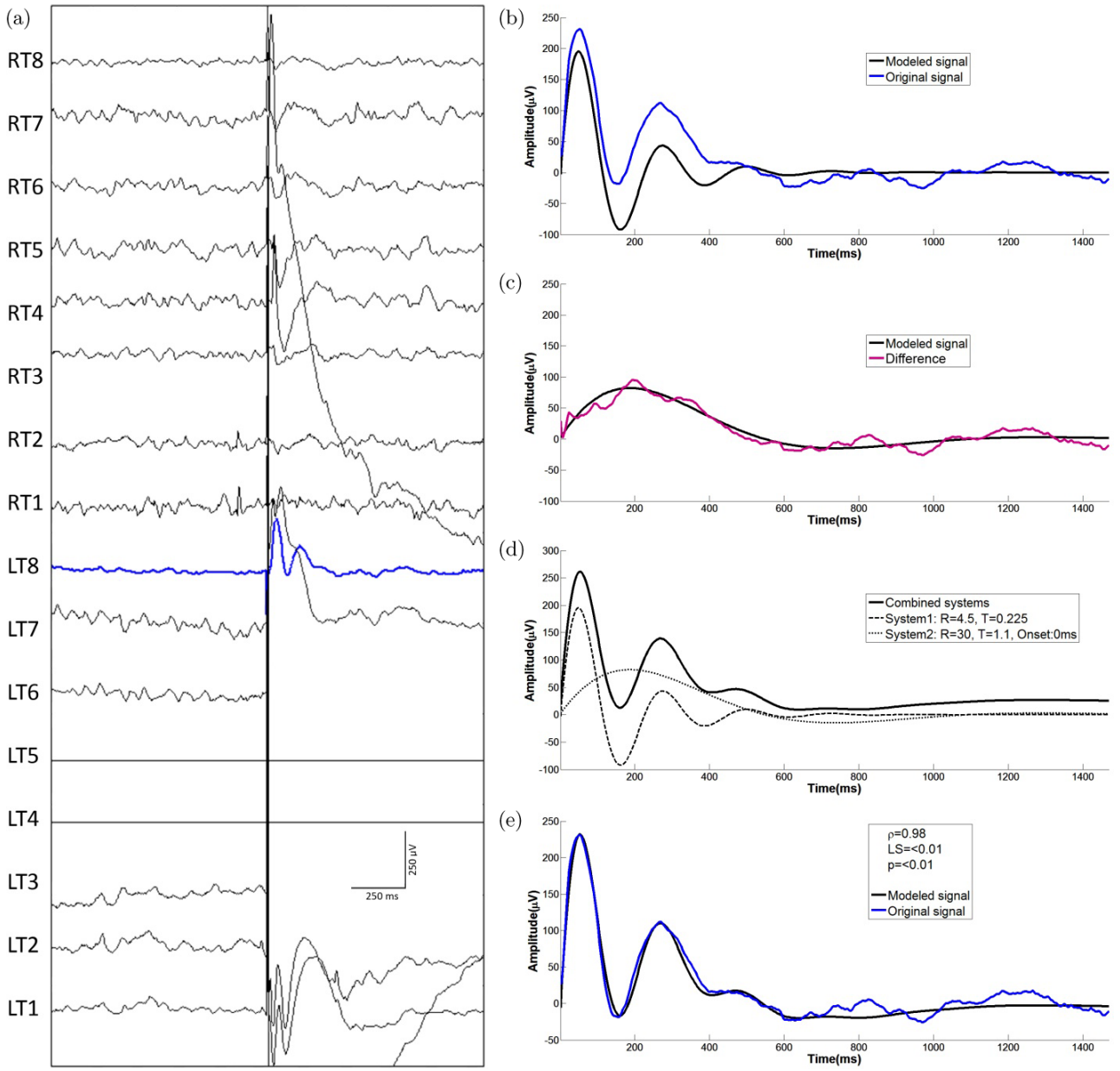

Fig. 2. (Color online) Modeling process. Patient implanted with subtemporal strips. (a) Averaged responses to SPES delivered between electrodes LT4 and LT5 (flat traces). Note the high amplitude artifact recorded at channels close to the two stimulating electrodes. Response in channel LT8 (blue trace) has been selected for modeling. (b) Recorded response (blue) and first control model (black). (c) Difference (purple) between recorded response and first control model obtained in (b), and the control system used to model the difference (second control model shown in black trace). (d) Recorded response (solid line), first control system model (thick dotted line) and second control system model (thin dotted line). (e) Comparison between recorded EEG response (blue line) and the final compound model (black line) obtained by adding first and second control models. RT: Right temporal, LT: Left temporal, R = Subsidence ratio, T = Period, ρ = Correlation coefficient, LS = Least square difference, p = significance.

in all cases. The amplitude of the models was automatically adjusted to obtain the lowest square difference between recorded response and model. In the last step, both models were added to obtain the ***final model*** which was compared with the original recorded response [Fig. 2(e)]. The degree of resemblance between final model and recorded response was quantified using Pearson correlation coefficients

(ρ) and square difference. The significance level for the correlation coefficient was defined as $p < 0.01$. Only those signals reaching a ρ value >0.8 and $p < 0.01$ were considered similar. As explained in the Appendix, all systems involved in modeling are second-order linear control systems. Thus, the terms "first" and "second" control systems refer to the fact that the first control system is the first system calculated to fit the response and also it is calculated from the first deflections on the recorded response. The second control system, if needed, is the second model calculated from the difference between the recorded response and the first control system.

2.8. *Modeling spontaneous EEG from responses to stimulation*

For each averaged response, bode diagrams reflecting the frequency-response for each control system were calculated and the peak resonance frequency identified (i.e. the frequency showing the highest gain). In addition, for each channel, the power spectrum of spontaneous EEG activity during the 20 s epoch previous to the first stimulation was calculated.

For each recording channel, Bode plots resulting from responses induced by stimulation applied to different sites were superimposed in order to compare them with frequency composition of the spontaneous EEG recorded in the same channel.

At a later stage, a grand average of Bode plots was carried out for each patient. All the obtained frequency-response Bode graphs from all channels were superimposed and the upper envelope of the graphs was calculated. The hypothesis was tested that the power spectrum of the EEG can be estimated as the summation of all resonance frequencies from all active connections. However, the summation of all the recorded Bode plots renders a rather spiky graph since a relatively low number of connections are available for study due to the necessarily limited number of electrodes implanted. The envelope of the Bode plot peaks was used to integrate (summate) all the Bode plots, because the connections where no electrodes were implanted were not studied and were therefore missing. The envelope was used as a way to smooth the curve and allow for the Bode plots from missing connections, thus improving the estimation of the spontaneous EEG. A 50-sample moving average (smoothing) was applied to the resulting envelope. The smoothed envelope was then superimposed to the average of the frequency composition of the spontaneous EEG from all channels from the same patient. Pearson correlation coefficients (ρ) were obtained in order to quantify the degree of resemblance between averaged power spectrum composition of the spontaneous EEG and the envelope of the Bode plots from all stimulations. Amplitudes of the Bode plot envelope were adjusted so that its maximal amplitude coincided with that of the power spectrum of the spontaneous EEG.

Sometimes resonance peaks in SPES Bode plots were observed which were not present in the power spectrum of the analyzed sample of spontaneous activity. It was hypothesized that such peaks in the SPES Bode plots were due to oscillatory mechanisms which were either: (a) Not active (or suppressed) during the sample of spontaneous EEG analyzed (for instance, alpha activity not present with eyes open), or (b) Their activity was too brief to be observed on the relatively long period of spontaneous EEG analyzed with power spectrum (for instance, occasional interictal epileptiform discharges or sharp waves). When such discrepancies between Bode plots and spontaneous power spectrum were observed, the complete telemetry record was reviewed in search of epileptiform discharges, sharp waves or oscillatory activity not present in the 20 s EEG sample selected for power spectrum. If found, the frequencies of oscillatory activity and of epileptiform discharges (inverse of their average duration) were measured to establish if they coincided with the unexplained resonance frequencies in the SPES Bode plots at the same location. If frequencies coincided, it was assumed that SPES could identify the oscillatory mechanisms of the region even if their resulting oscillations were not observed in the 20 s EEG sample selected for power spectrum.

2.9. *Statistics*

Kolmogorov–Smirnov and Shapiro–Wilk tests were used to assess if variables are normally distributed within groups. Kruskal–Wallis H test was used to determine if there were statistically significant differences between different groups of variables. A Mann-Whitney U test with Bonferroni correction (p value was defined as <0.01) was performed to find specific differences between groups for the parameters that showed significant differences.

3. Results

3.1. *Patients*

The study included artifact-free intracranial SPES responses from five patients (2 males, 3 females, mean age = 30.6 years, range between 23 and 40 years) who underwent temporal lobectomy for the treatment of their epilepsy and became seizure free after surgery, with follow-up periods between 12 and 36 months. Four patients (P1–P4) had temporal subdural strips and one patient (P5) had depth electrodes implanted (Fig. 3).

3.2. *Distinction between response and stimulation artifact*

In order to distinguish between stimulation artifact and cortical responses, an *in vitro* recording was carried out using gauze soaked with saline as a model for an inert conductor resembling the passive electrical properties the brain. Figure 4 compares recordings obtained *in vitro* and in a patient. Note the additional deflections (arrows) occurring after the artifact only in patient recordings, hence demonstrating that these are biological responses rather than artifacts.

Apart from overall morphology and amplitude, an additional criterion used to separate biological responses from stimulation artifacts was that the polarity of biological responses does not change with changes in current polarity between the two stimulating electrodes, whereas the polarity of stimulation artifacts changes with changes in current direction between the stimulating electrodes.

3.3. *Evaluation of model parameters*

When an SPES response was present, signals were modeled following the procedures described in the methods section in order to define the existence of one or two control systems and their parameters.

We found that a response could be equally modeled as an open ($K = 0$) or close loop ($K \neq 0$) system (Fig. 5). Therefore, in order to reduce the number of parameters involved, open loop systems were used for modeling in the remaining of the paper.

Responses to SPES showed variability in morphology. When more than one deflection was present,

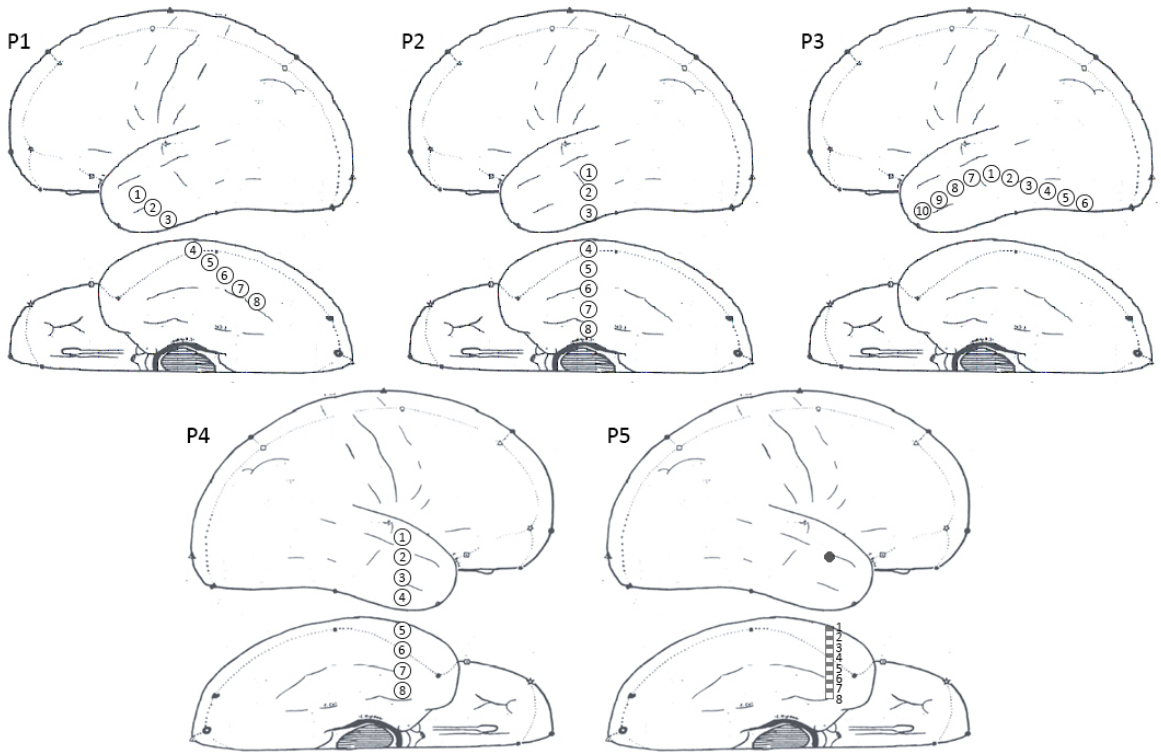

Fig. 3. Electrode implantations in the "non-epileptogenic" temporal lobe. Patients 1–4 had subdural electrodes whereas patient 5 had depth electrodes.

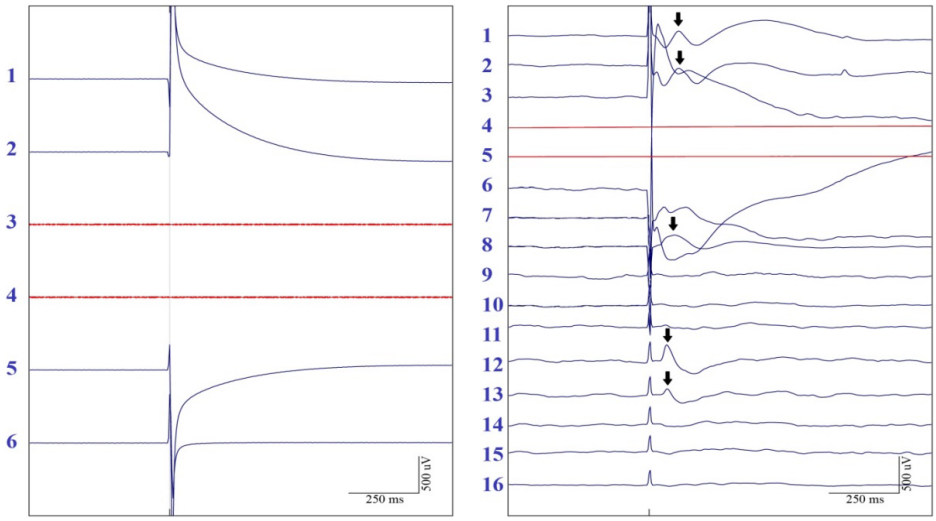

(a) (b)

Fig. 4. *In vitro* versus *in vivo* recordings. SPES in saline (a) and in a patient (b). Note the presence *in vivo* of additional deflections after the stimulus. Biological responses to SPES, no present *in vitro*, are marked with arrows.

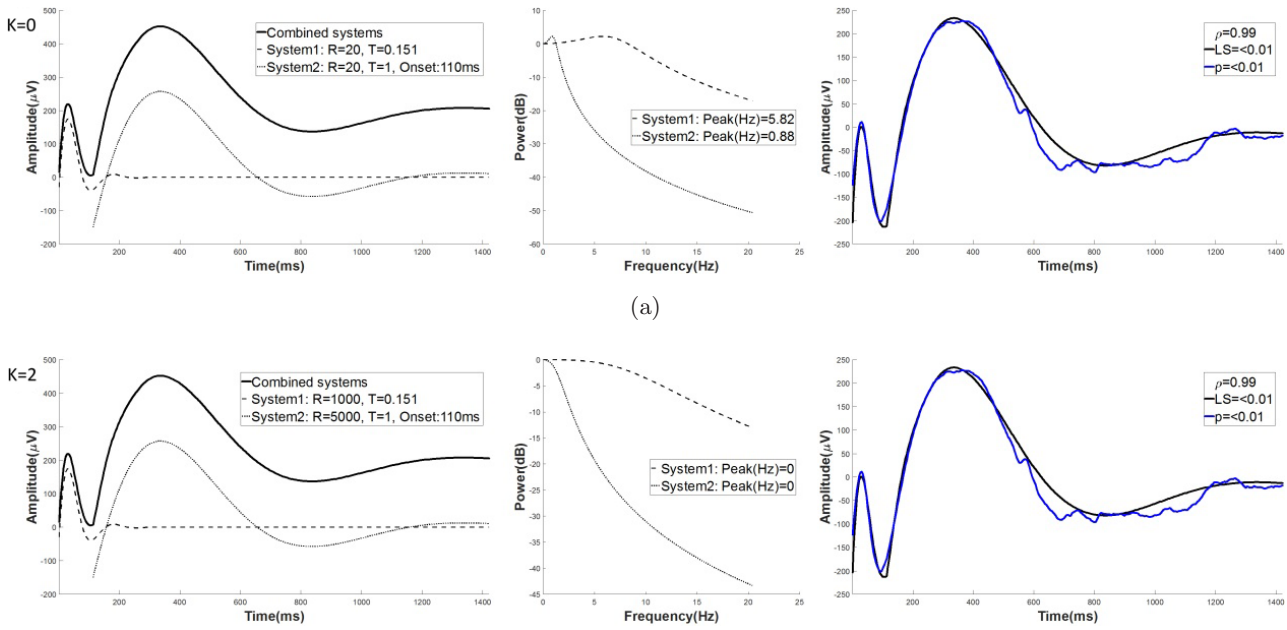

(a)

(b)

Fig. 5. Modeling the same recorded response (black trace) with open (a) and closed (b) loop control systems. The figure shows the decomposition of the response in first and second systems in the time domain (left column), in the frequency domain (Bode plots, middle column) and the combination of both systems into the final model of the response (right column). Note that identical first (dash trace in left and middle columns) and second (gray trace in left and middle columns) control systems can be obtained with different combinations of K and R which render identical final models (right column). A higher R is translated into higher attenuation values on the frequency spectrum and a blunted resonance peak.

deflections tended to show higher duration with longer latency, e.g. late deflections were longer than earlier ones (see example in Fig. 5). This could not be modeled by a single linear control system but could be due to the presence of two control systems. This is the main reason why we embarked in modeling with more than one control system in the same response.

3.4. *SPES responses*

Out of 204 total recording channels, 121 channels showed responses to 32 stimulation sites. 30% of recording channels showed large stimulus artifact which obscured the EEG response (Table 2) and were always located in the vicinity of the pair of stimulating electrodes. 9.8% of channels failed to show a response.

Four response types have been identified and are illustrated in Fig. 6. In summary, the four types can be described as follows:

(a) A single short surface-negative response of short duration lasting for less than 250 ms.
(b) A longer surface-negative response lasting for longer than 250 ms.

Table 2. Response types. Channels and responses are displayed in relation to the approximate distance to the stimulating electrodes.

	Type							
Distance (mm)	A	B	C	D	No response	Stim artifact	Other artifacts	Total
<10	10	2	1	6	—	53	—	72
10–20	6	7	4	18	3	10	—	48
20–30	5	4	2	19	8	—	—	38
30–40	1	1	—	14	3	—	1	20
40–50	2	1	2	9	4	—	—	18
50–60	—	—	—	3	1	—	—	4
60–70	1	1	—	2	—	—	—	4
Total	25	16	9	71	19	63	1	204

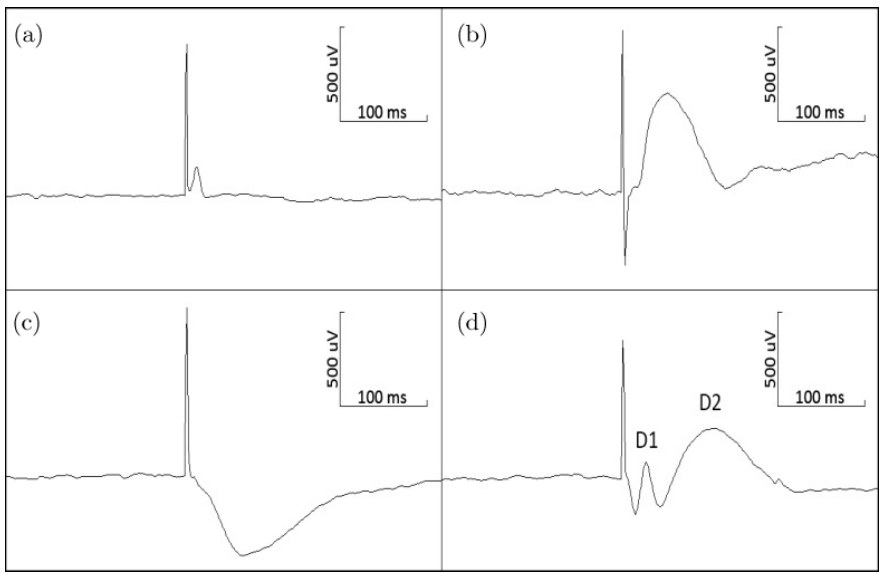

Fig. 6. Typical responses. Examples (a), (b) and (c) illustrate responses with a limited number of deflections (high R value) which are the simplest types of observed responses. Responses with more deflections illustrated in (d) can be considered as a combination of responses (a) and (b) (see text).

(c) A long surface-positive response, similar to type B but with opposite polarity.
(d) Combination of morphologies described above.

In as many as 71/204 (35%) of channels, two different superimposed responses of types A–C could be identified (D), which could be modeled as two different control systems. Their initial deflections showed shorter components resembling type A responses (D1) followed by later slower components similar to type B responses (D2). No surface-positive deflections (type C) were

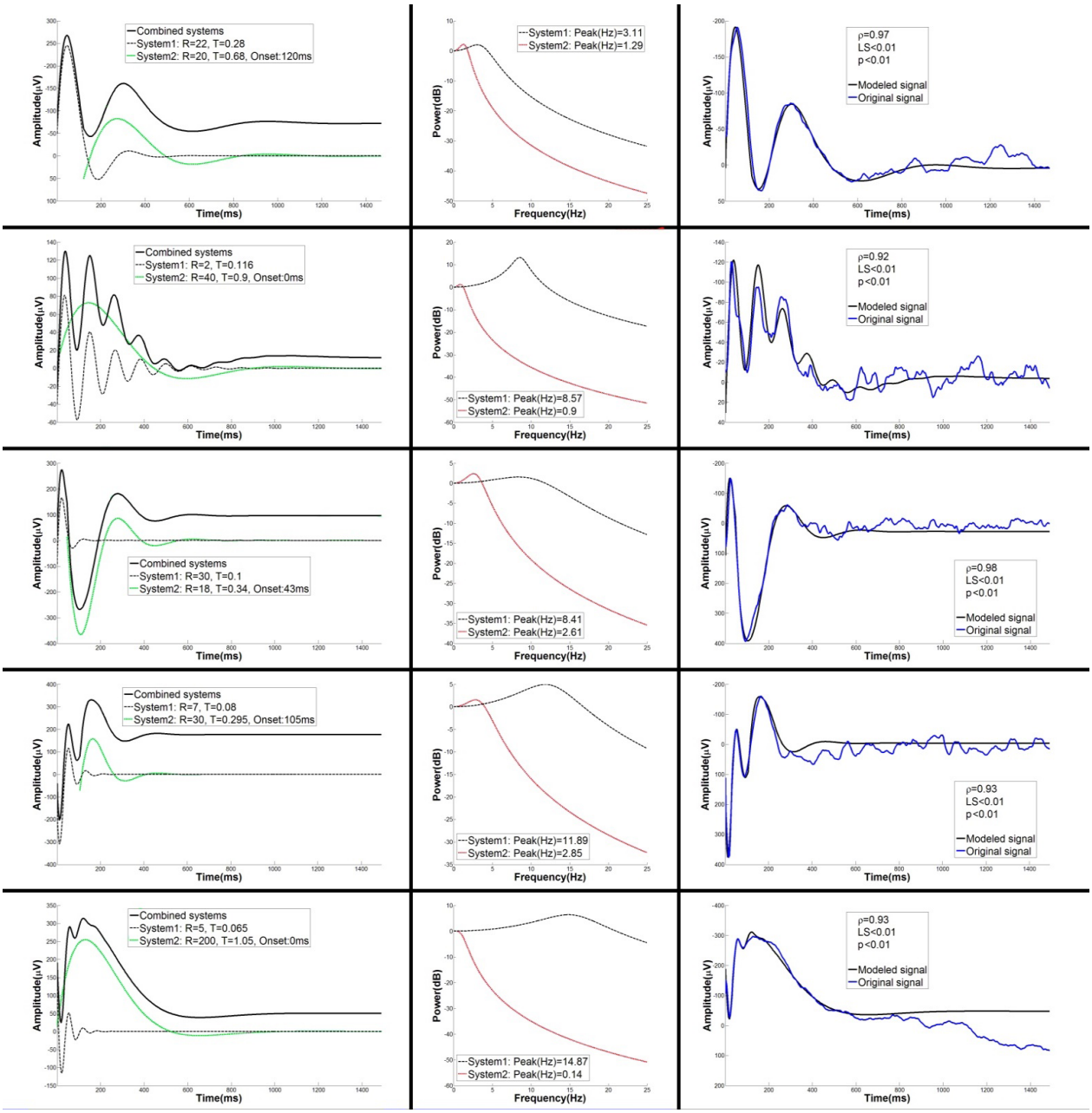

Fig. 7. (Color online) Modeled and original responses to SPES. Left column: Examples of responses (solid black line) modeled as the combination of two control systems (dashed black and green lines). Middle column: Bode plots for the control systems from each modeled response (dashed black and red lines). Right column: Overlapped original (blue line) and modeled (black line) signals. R = Subsidence ratio, T = Period of the oscillation, ρ = Correlation coefficient, LS = Least squares difference.

Table 3. Median and interquartile range values (brackets) for latency, amplitude, period and distance to the stimulating electrode values within each group. T = Period, R = Subsidence ratio.

Group	n	Onset latency (ms)	Peak latency (ms)	Amplitude (μV)	$T(s)$	Distance (mm)	R
A	25	15.00 (15.00)	59.06 (41.01)	155.45 (142.38)	0.12 (0.075)	20.00 (20.00)	40.00 (50.00)
B	16	30.00 (88.00)	199.65 (91.57)	124.03 (179.94)	0.49 (0.23)	20.00 (10.00)	10.00 (20.00)
C	9	20.00 (58.00)	238.53 (157.3)	278.75 (152.58)	0.55 (0.50)	20.00 (22.50)	200.00 (190.00)
D1	71	12.00 (30.00)	60.78 (46.87)	144.36 (128.09)	0.14 (0.09)	30.00 (20.00)	20.00 (25.00)
D2	71	80.00 (150.00)	262.19 (137.54)	119.44 (131.35)	0.60 (0.37)	30.00 (20.00)	20.00 (45.00)

observed when two components were identified (type D).

Among artifact-free responses (59.3%) recorded in a given channel, a single control system could model the response in 41.3% and two systems were required in 58.7%.

3.5. *Modeling of SPES responses*

Averaged SPES responses were modeled following the process described in methods section (Figs. 2 and 5). As stated above, a single control system was identified in 50 responses and two control systems in 71 responses. Similarity between recorded responses and modeled responses was quantified. Traces reaching ρ values above 0.8 with statistical significance <0.01 were obtained in 79.04% of responses. ρ values of 0.9–1 were obtained in 55.65% of responses, ρ values between 0.8 and 0.9 in 23.39%, between 0.7 and 0.8 in 11.29%, between 0.6 and 0.7 in 3.23%, between 0.5 and 0.6 in 3.23%, and less than 0.5 was obtained in 3.23% of responses.

Five examples of modeled responses requiring two control systems are shown in Fig. 7. The left-hand column shows the recorded response superimposed on the two control systems required to model it. The middle column shows the Bode diagrams for the two control systems, showing that each system has a frequency with largest amplitude, i.e. the resonance frequency. The right column shows recorded and modeled responses superimposed.

3.6. *Properties of responses*

Table 2 shows response type according to distance from recording to stimulating electrodes. Type A tends to occur closest to stimulating electrodes whereas types B and C are more common at 10–20 mm from the stimulating electrodes. Compound responses (type D) were the most common and widespread, showing maximal incidence around 20–30 mm from stimulating electrodes. Table 3 shows parameters (peak latency, amplitude, period and distance between stimulating and recording electrodes) of the different response types (A, B, C, D1 and D2). Variables were not normally distributed within each group (Kolmogorov–Smirnov and Shapiro–Wilk tests).

Significant differences were found in onset latency, peak latency, amplitude, T and distance values between response types (Kruskal–Wallis H test, onset latency $\chi^2(2) = 72.117, p = 0.000$; peak latency $\chi^2(2) = 137.150, p = 0.000$; amplitude $\chi^2(2) = 10.283, p = 0.036; T\chi^2(2) = 122.842$, $p = 0.000$; distance $\chi^2(2) = 14.121, p = 0.007$). Mean values for these parameters within each group are displayed in Table 3.

No significant differences were found between the different types of responses in terms of R values (Kruskal–Wallis H test).

A Mann–Whitney U test with Bonferroni correction (p value was defined as <0.01) was performed to find specific differences between groups for the parameters that showed significant differences (amplitude, period and distance) (Table 4).

The only significant difference in amplitude was found between C type and all other groups except type B (Mann–Whitney U test with Bonferroni correction). In terms of period and peak latency, there were no significant differences between A and D1, which were significantly different from B, C and D2 types. Similarly, B, C and D2 types did not show significant differences among themselves but reached statistical significance when compared to A or D1. With regards to distance to stimulating electrode,

Table 4. Statistical significance of Mann–Whitney U with Bonferroni correction ($p < 0.01$).

	Onset latency				
Group	A	B	C	D1	D2
A	—	0.000*	0.073	0.413	0.002*
B	0.000*	—	0.250	0.003*	0.151
C	0.073*	0.250	—	0.102	0.007*
D1	0.413	0.003*	0.102	—	0.000*
D2	0.002*	0.151	0.007*	0.000*	—
	Peak latency				
Group	A	B	C	D1	D2
A	—	0.000*	0.000*	0.312	0.000*
B	0.000*	—	0.643	0.000*	0.234
C	0.000*	0.643	—	0.000*	0.110
D1	0.312	0.000*	0.000*	—	0.000*
D2	0.000*	0.234	0.110	0.000*	—
	T				
Group	A	B	C	D1	D2
A	—	0.000*	0.000*	0.255	0.000*
B	0.000*	—	0.926	0.000*	0.491
C	0.000*	0.926	—	0.000*	0.945
D1	0.255	0.000*	0.000*	—	0.000*
D2	0.000*	0.491	0.945	0.000*	—
	Distance to stimulation				
Group	A	B	C	D1	D2
A	—	0.091	0.274	0.001*	0.006*
B	0.091	—	0.734	0.265	0.333
C	0.274	0.734	—	0.266	0.320
D1	0.001*	0.265	0.266	—	0.817
D2	0.006*	0.333	0.320	0.817	—
	Amplitude				
Group	A	B	C	D1	D2
A	—	0.968	0.005*	0.575	0.027
B	0.968	—	0.011	0.644	0.887
C	0.005*	0.011	—	0.005*	0.002*
D1	0.575	0.644	0.005*	—	0.377
D2	0.027	0.887	0.002*	0.377	—

only significant differences were found between D1–D2 and A.

In summary, there were no significant differences in terms of latency, amplitude and period neither between A and D1 types or between B and D2 types. C type was not significantly different to B and D2 types in terms of latency, period and distance to the stimulating electrode, but amplitude values were significantly different. This suggests that A responses and the first component of D responses can be considered equivalent and so can be B responses and the second component of D responses.

For the sake of completeness, Table 5 shows the equivalence between previously described peak nomenclature and the control systems described in the present work.

3.7. *Modeling spontaneous oscillations*

For each patient, the power spectrum of the spontaneous EEG and Bode plots for each control model were obtained and calculated following the procedure described in the methods section. Figure 8 shows the Bode plots from all stimulations inducing a response in each channel (blue) and the power spectrum of the spontaneous EEG of each channel (red) for patient 2. The peaks of resonance in the Bode plots tend to occur within the frequency range of most activity on the spectrum of the spontaneous EEG (red), suggesting that the cortex tends to oscillate at the resonance peaks shown by the Bode plots of SPES responses.

Furthermore, in some channels (e.g. E3 and E4), the largest frequency on the Bode plot corresponded to specific peaks on the power spectrum (arrows in Fig. 8).

The clustering of resonance frequencies in the Bode plots of the responses around the frequencies showing larger power in the spontaneous EEG raised the question of whether the power spectrum of the spontaneous EEG can be estimated by the addition of the resonance frequencies from all regions projecting to the region where the EEG is recorded. In other words, resonance frequency from each Bode plot would show the frequency at which each connected site contributes to the spontaneous EEG of the region.

The number of electrodes implanted is necessarily limited. Consequently, it is not possible to know the Bode plot from all regions connected to any given one.

The suggestion is that if we had more electrodes with more responses, we will end up with a higher degree of similarity between the compound Bode plot and the power of the spontaneous EEG spectrum

Table 5. Median values and interquartile ranges for latency, amplitude, period and distance to the stimulating electrode values within each group. T = Period, R = Subsidence ratio.

Type		Onset latency (ms)	Peak latency (ms)	Amplitude (μV)	R	$T(s)$	Distance (mm)
N1 (A/D1)	Median	13.5	59.92	145.48	20.00	0.14	30.0
	Interquartile range	20.00	43.12	133.36	43.75	0.09	20.0
N2 (B/D2)	Median	70	249.49	121.70	20.00	0.55	30.0
	Interquartile range	155	124.49	132.07	42.00	0.34	20.0
P1 (C)	Median	20.00	238.53	278.75	200.00	0.55	20.0
	Interquartile range	58.00	157.3	152.58	190.00	0.50	22.5

by increasing the number of connections studied, we calculated a grand average of power spectra from all channels and superimposed the envelope of all Bode plots from all channels (the compound Bode plot) for each patient (Fig. 9). The averaged power spectrum and the compound frequency response curves in the Bode plots were similar in all five patients showing Pearson correlation coefficients above 0.9 ($p < 0.01$).

Despite the overall similarity between power spectra and compound Bode plots seen in Fig. 9, some channels revealed isolated peaks in the frequencies of the compound Bode plot (arrows in Fig. 9) not corresponding to similar peaks in the compound power spectrum of the spontaneous EEG. Table 6 shows frequency and periods of the Bode plot peaks that do not appear in the power spectrum of the spontaneous EEG (unexplained peaks). The complete telemetry record was reviewed to find elements to explain such discrepancies. In all patients, there was either alpha activity or interictal activity at surprisingly similar frequencies to the unexplained Bode plot peaks, therefore providing an explanation for the Bode plot peaks not present in the power spectrum.

In patient 1, the SPES responses responsible for the extra peak (at a frequency of 9.6 Hz) on the compound Bode plot were generated by the most posterior electrodes (electrodes 7 and 8 in Fig. 3). This is the region showing alpha activity at 9–10 Hz on eye closure, even though such activity was not present in the initial 20 sample of spontaneous EEG which was obtained with eyes open.

Patients 2–5 showed unexplained peaks on their compound Bode plots with frequencies at 7.1, 13.6, 11.8 and 15.2 Hz (i.e. periods corresponding to 140, 74, 84.7 and 66 ms, respectively). The four patients showed epileptiform discharges (spike wave discharges or sharp waves) of similar durations (periods at 144, 86, 86 and 70 ms, respectively) which explained the corresponding peaks on the compound Bode plots (Fig. 10).

Patients 3 and 4 showed additional interictal discharges with durations of 300 ms and 62 ms, respectively, corresponding to frequencies (3.33 Hz and 16.13 Hz, respectively) outside the unexplained peaks for the same patients.

4. Discussion

We essentially describe a method to characterize connections and how they can contribute to spontaneous oscillations. We found it useful in explaining how connections contribute to the oscillatory nature of the spontaneous EEG generated in the regions were electrodes were implanted. Our results suggest that cortical interactions can be described as linear control systems. Responses to electrical stimulation can be explained as the superimposition of responses from one or two control systems which can be described with only 3–6 parameters (R, T and delay-phase for each control system). This method can characterize responses regardless of whether they show the standard deflexions and the method can be used to describe waveforms with few parameters. More importantly, the method can quantify the resonant frequency of functional coupling between two sites, and we suggest that the models can explain spontaneous EEG oscillations, teasing out the relative contributions to spontaneous oscillations from each pair of connected regions. Furthermore, the method appears to be able to identify oscillatory capabilities of the different regions of the cortex, potential oscillations which may not be present in

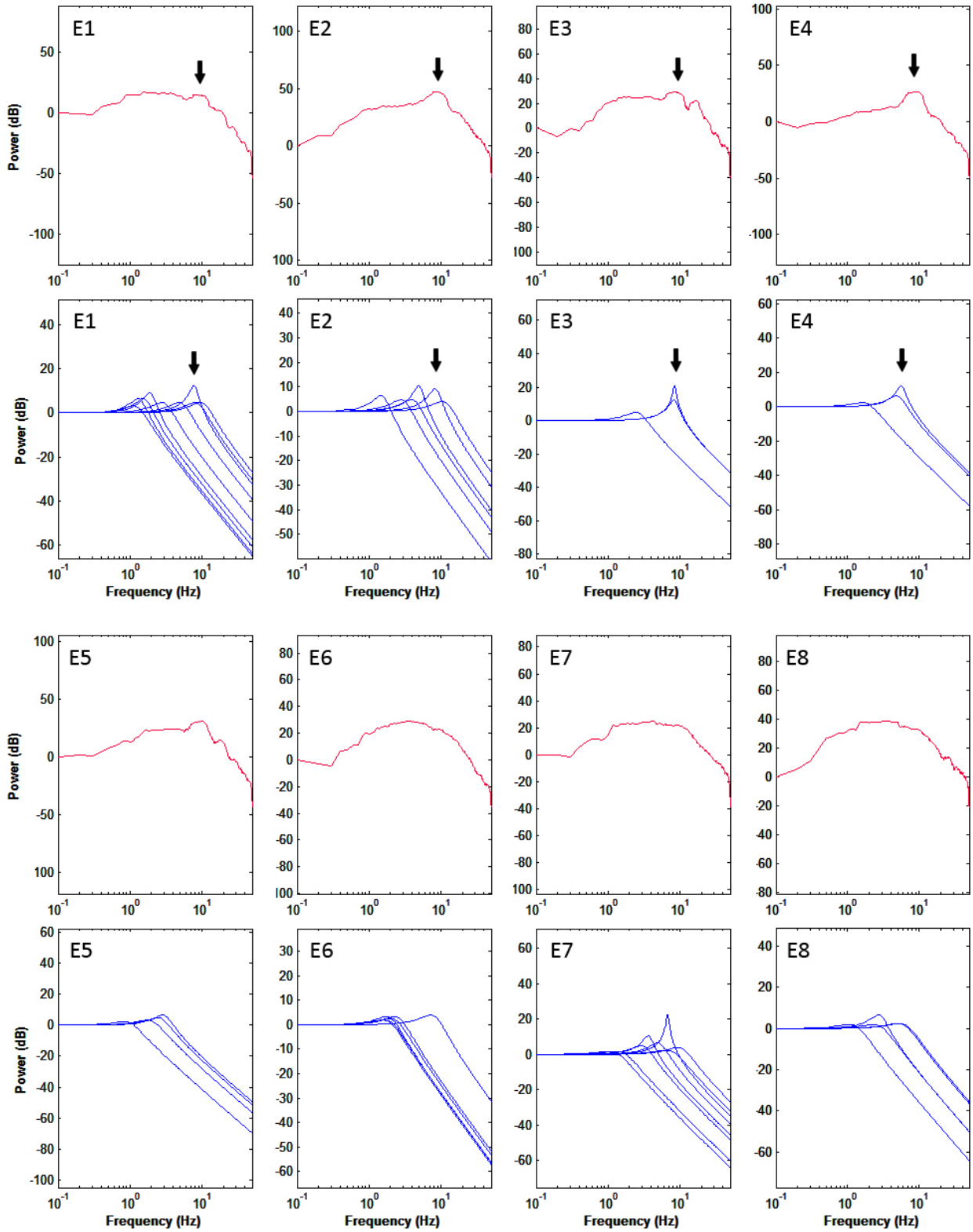

Fig. 8. (Color online) Example of spontaneous oscillations modeling in patient 2. Diagrams showing the power spectrum of spontaneous EEG activity contained within the 20 s epoch previous to the first electrical stimulation for each channel (red) and the frequency response Bode plots for each control system (blue) identified for each electrode in patient 2. Note that some of the largest Bode plot peaks appear on the spontaneous EEG spectra as indicated by the inserted arrows.

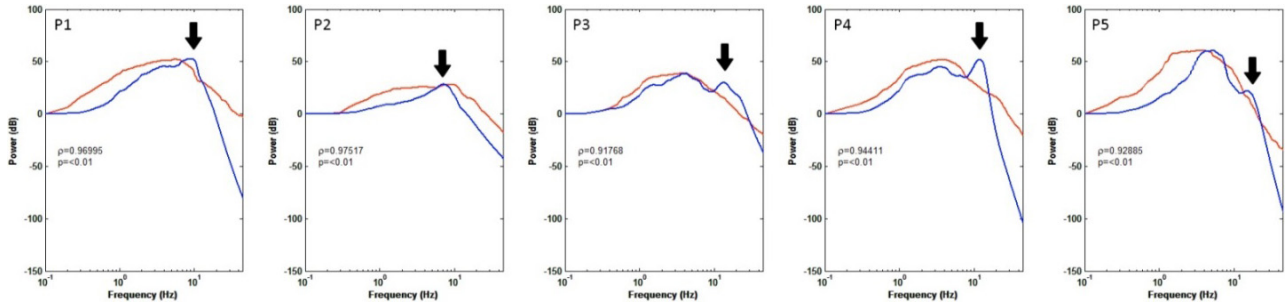

Fig. 9. (Color online) Compound power spectrum versus compound frequency response curves (compound Bode plot). For each patient, the red curve shows the averaged power spectrum from the spontaneous EEG for all channels (the compound power spectrum). The blue curve shows the addition of all Bode plots from all stimulation (i.e. the compound Bode plot) which represent the frequency response curves induced by all stimulations. The latter was computed by superimposing the Bode graphs from all channels and calculating the upper envelope of the graphs. A moving average was applied to the resulting envelope. Note that, despite their similarity, each patient showed peaks in the compound Bode plots (black arrows) which were not present in the compound power spectrum of the spontaneous EEG.

Table 6. Compound Bode plot peaks to be explained in each patient and EEG elements that justify them.

Patient	Peak to be explained (frequency in Hz or period in ms)	Electrode number showing the peak to be explained	EEG element that explains the peak	Topography of EEG element that explains the peaks	Other elements in the spontaneous interictal EEG
1	9.6 Hz or 104 ms	Post temp-occipital (7–8)	Alpha activity at 9–10 Hz	Maximal at electrodes 7–8	—
2	7.1 Hz or 140 ms	Electrode 7	Interictal spike wave discharge with period of 144 ms	All channels but maximal at electrode 7	—
3	13.6 Hz or 74 ms	Electrodes 1, 2	Interictal sharp waves with period of 86 ms	Maximal at electrode 2	Sharp waves of 300 ms maximal at electrode 10
4	11.8 Hz or 84.7 ms	Electrodes 3, 6	Interictal sharp waves with period of 86 ms	Electrodes 1–5 Maximal at electrode 4	Spike-wave of 62 ms at electrodes 6–8
5	15.2 or 66 ms	Electrodes 1, 8	Interictal spikes with period of 70 ms	Electrode 8	—

an actual record of spontaneous EEG. This may be particularly relevant to predict, during the interictal period, impending seizures or the regions originating seizures as these are characterized by transient oscillatory behavior. Data were obtained from the non-epileptogenic hemisphere in patients becoming seizure-free after surgery in order to maximize the chances of studying less abnormal brain tissue within the temporal lobe.

The principles of our proposed method are simple to understand. In essence, electrical stimulation activates functional coupling between connected regions, inducing cortical oscillations at the frequencies at which the regions involved are most likely to oscillate. The frequencies at which a connection is likely to oscillate after stimulation determine the largest peaks on the frequency response of the connected regions (the resonance frequencies) and the resonance frequencies of the local connections will determine the overall oscillatory behavior of the region. In this context, it is easy to understand that interictal epileptiform discharges or seizures can arise when the resonance frequency of one connection dominates over others, and our method could, in principle,

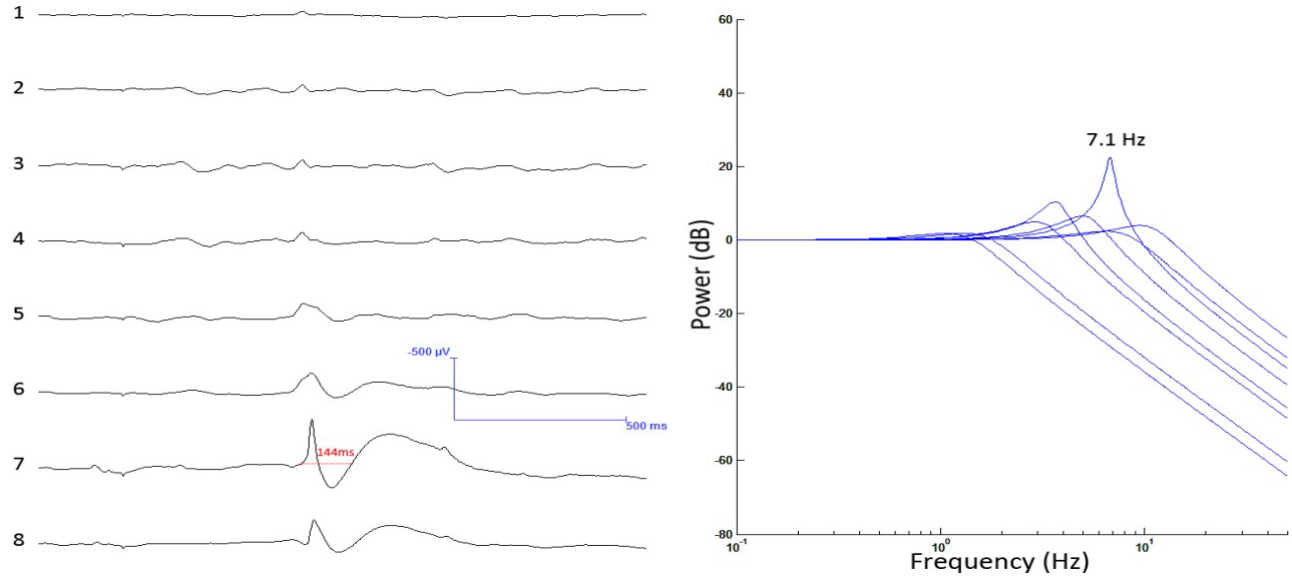

Fig. 10. Patient 2. Left, averaged interictal discharge largest at electrode 7 showing duration of 144 ms (determining a frequency of 1/0.144 or 6.94 Hz). The frequency of this discharge is close to the largest peak (at 7.1 Hz) present in the Bode plots of SPES responses (right) which were recorded at the same electrode 7. Such interictal discharges were not present in the initial 20 s sample of spontaneous EEG. However, their frequency was prominent in SPES responses recorded by the same electrode, suggesting that the capacity of the corresponding connections to generate such discharges could be inferred from responses to stimulation, since the observed frequency peak is consistent with location and frequency with the interictal discharges.

measure such dominance. This is a new way to interpret the EEG and cortical physiology in general, which opens a wide new area of research in neuroscience by providing objective measures of degree of functional coupling between connected regions in the amplitude and frequency domains.

4.1. *Control system models and cortical dynamics*

Brain dynamics display non-linear features (e.g. the behavior of single neurons) in conjunction to linear characteristics (e.g. Weber's law, the sinusoidal behavior of alpha and sigma activities). More specifically, the amplitude of early responses behaves broadly linearly over a range of amplitudes,[15,29] suggesting that linear models may be adequate for characterization of the amplitude of response oscillations. In any case, in the end, the main purpose of our method is the characterization of brief oscillations with few parameters. The linear models used have been effective for this purpose. Overall, the findings from this study are consistent with clinical practice. The EEG itself can be described as a low-pass filter in that the amplitude of oscillations decreases with increasing frequency as shown by the power spectrum of spontaneous EEG activity. Accordingly, the Bode plots obtained describe the response of the modeled system to any frequency. Above the cut-off frequency, Bode plots show higher signal attenuation the higher the frequency. Each Bode plot shows an amplitude peak at the so-called resonance frequency, presumably the frequency which is easier to generate by the system.

We have treated the stimulus as a unit step function, when in fact it would be better described as a unit impulse function. Indeed, responses are transient oscillations returning to 0. It would be impossible to apply a true step function to the cortex as this would polarize the cortex for long enough to possibly induce tissue damage. Conceptually we could consider that each single pulse activates the neuronal network for a while, maintaining it on an activated state, which in itself could be considered as a pseudo-step function. The difference between considering the stimulus as a step or impulse function would probably be minimal, as we are essentially interested in characterizing the frequency of the resulting brief oscillations, and the method used appears effective for this purpose. The practical difference is that the

mathematical development (appendix) is simpler for the step function.

Figure 9 suggests that the frequency composition of the spontaneous EEG can be predicted from the summation of the frequency responses from individual connections (compound Bode plots). In other words, the transfer functions of the corresponding control systems summate to generate cortical activity. This means that the control systems from different connections are largely arranged in parallel rather than in series since the transfer functions of control systems arranged in parallel add up. The overall similarity found between traces shown in Fig. 9 (showing Pearson correlation coefficients above 0.9, $p < 0.01$) despite the limited number of electrodes was very surprising and suggests that the study with more electrodes will increase such similarity.

Some peaks in the compound Bode diagram were not present in the power spectrum of the spontaneous EEG. Such peaks were found to be similar to the frequency of alpha activity or the instantaneous frequency of interictal epileptiform discharges recorded at the appropriate channel. Since the spontaneous EEG selected for power spectrum was obtained with eyes open (alpha activity blocked) and epileptiform discharges are too brief to be observed in the power spectrum of a 20 s EEG, it is not surprising that their frequencies do not appear in the power spectrum of the spontaneous EEG, yet they are shown by the SPES Bode plots. Therefore, Bode plots obtained from responses to SPES could be a biomarker for the capacity of the cortex to generate activity which may or may not be present in the specific sample of EEG.

A puzzling finding is that despite their overall similarities the blue traces appear to be slightly shifted to the right (toward higher frequencies) than the red traces in Fig. 9. This may be due to the fact that pairs of neurons in driven neocortex have a shorter length scale than those found in spontaneous activity.[37,38] Alternatively, this discrepancy could be explained by distortions in the stimulus step function induced by the resistance-capacitance properties of the brain tissue.

It could be claimed that the spectra of the spontaneous EEG shows very broad bandwidth, and this is why the sharp peaks in Bode plots are within the frequency range of the spontaneous EEG. As shown in Figs. 8 and 9, most EEG activity occurs below 12 Hz. The graph falls off thereafter and has therefore been omitted in the figures. The assertion that this band below 12 Hz is "broad" is subjective. One could equally take the opposite view, that it is extremely narrow. If the duration of action and postsynaptic potentials are 1–2 ms, electrical activity could in principle oscillate at up to 500–1000 Hz. The fact that most power is below 12 Hz can be taken as evidence that the band is surprisingly narrow. The main point is that most Bode plot peaks scatter within this band and are not present outside it. Therefore, we suggest that the EEG could be considered as the addition of all individual resonance peaks from all connections. Even some of the largest resonance peaks in the individual Bode plots can be seen on the spontaneous EEG in Fig. 8.

4.2. *Physiological implications*

A very interesting observation was that late deflections tend to show longer duration than earlier deflections in nearly 60% of recorded responses [Figs. 5, 6(D) and 7]. This cannot easily be modeled with a single control system, requiring the superimposition of two control systems to accurately model the response. Although both systems add up to form the standard N1, P1 and N2 deflections, the earlier deflections are dominated by fast oscillatory system, whereas later deflections are dominated by the slower system. Not all deflections are present in all responses, suggesting a different generation mechanism for different deflections.[11,12,15,21] Indeed, simultaneous EEG and single cell recordings in animal and humans suggest that responses to SPES are composed of an earlier wave of excitation (lasting for less than 100 ms) followed by a longer period of inhibition (lasting for up to 700 ms).[28,39–41] Based on such duration for excitatory and inhibitory waves after stimulation, it would be tempting to speculate that the fast systems (such as responses type A and D1) tend to model excitation whereas the slower systems (such as responses B, C and D2) tend to model inhibition. Since interictal epileptiform discharges and responses to SPES show similar morphology and cellular mechanisms,[41,42] our method can also be used to model interictal epileptiform discharges.

Functional connectivity studies with SPES tend to concentrate on the study of presence or absence

of responses.[6,11,12,14,16–18,21–23] The implication has been that the presence of response at site A when stimulating at site B implied the presence of functional connections from B to A. For equal distance between stimulating and recording electrodes, it is assumed that the strength of the connections is proportional to response amplitude. Thus, SPES responses provide information on the presence, strength and direction of functional connections. However, it is unclear if the morphology of responses is related to the nature of the connections. Our method goes one step ahead in estimating the coupling frequencies between connected regions and the relative contribution of such coupling to the overall oscillatory activity. Consequently, we suggest that for a given recording site, our method could be used to tease out the relative contribution toward activity from each site connected to it, in addition to revealing the frequencies at which specific connections are capable of oscillating or most likely to oscillate. The damped oscillatory responses described here appear to be rather ubiquitous, possibly a manifestation of some generic cortical mechanism, suggesting that the method proposed could be used to model other electrical responses such as somatosensory evoked responses or high-frequency oscillations. Furthermore, it appears that our method can detect the capability of a region to generate frequencies which may not be present in a sampled EEG record as suggested by Table 6. For instance, the ability to generate alpha activity by temporo-occipital cortex was identified on the SPES Bode plots even when the sampled EEG and SPES responses were recorded with eyes open and did not show alpha activity (patient 1). The compound Bode plot for SPES responses showed a peak at the frequency of the alpha activity of that patient at the most posterior electrode which is precisely the electrode that recorded alpha activity when eyes were closed. An interpretation may be that SPES responses at the posterior electrode contain the alpha frequency because the underlying cortex is capable of generating alpha activity even if the brain was not actually generating alpha during the recording. Similarly, the capability to generate frequencies present in epileptiform discharges may have been identified by the method even when discharges were not present in the spontaneous EEG sampled (patients 2–5). The power spectrum of the EEG is unlikely to show a peak at the frequency of epileptiform discharges because discharges are either absent or very brief (one or few discharges lasting for 400 ms will be diluted in the power spectrum of a 20 s EEG). However, the frequencies of the discharges appear in the compound Bode plot at the appropriate channels. In fact, this finding is not all that surprising because we have described that SPES responses resemble the epileptiform discharges seen in the same channel.[42] A puzzling finding is that there where two patterns of epileptiform discharges which did not appear on specific peaks in the compound Bode plots (durations of 300 ms in patient 3, and of 62 ms in patient 4). This may reflect a limitation of stimulation with intracranial electrodes, since areas without implanted electrodes were not stimulated and consequently the frequency response of their connections not explored.

The question of whether this method could eventually be of use to draw conclusions about the normal brain is fascinating. Overall, the brain and EEG of people with and without epilepsy have many features in common. Consequently, findings obtained from the use of this method may unmask some of the mechanisms of normal phenomena (such as the generation of the alpha rhythm and sleep phenomena, see for instance Voysey *et al.* 2015[43]) which may contribute to our understanding of the oscillatory behavior of the non-epileptic brain in addition to that involved in generating seizures.

To conclude, we provide a method that describes the oscillatory behavior of the EEG in terms of control theory while estimating oscillatory coupling between connected cortical regions. It may have the potential to identify frequencies at which cortical regions are able to oscillate, and possibly to separate excitatory and inhibitory activities between regions. The method is unique in that it has the potential to bring together dynamic and network models as it provides information on connectivity as well as network interactions and behavior.

Appendix A. Mathematical Models

Second-order linear control models were developed and evaluated. Hereafter, $y(t)$ will describe the recorded response to stimulation whereas $y'(t)$ designates the modeled response of a control system.

This model assumes that human cortex can be described as a second-order control system.[27] Each

SPES pulse behaves as a unit step input (U) to the system. A generic response of such systems to a unit step function is shown in Fig. 1. The cortical response to SPES is regarded as the system output $[Y(t)]$. The response of the system to any frequency is determined by the response to a unit step function and will be displayed as standard Bode plots.

The transfer function $[G(s)]$ of a second-order open-loop (without feedback) control system is:

$$G(s) = \frac{O(s)}{I(s)} = \frac{\omega_n^2}{s^2 + 2\zeta\omega_n s + \omega_n^2}, \tag{A.1}$$

where $O(s)$ is the output (response); $I(s)$ is the unit step input; $s = j\omega$; j = square root of -1; ζ is the dimensionless damping ratio and ω_n is the cut-off frequency:

$$\omega_n = \frac{\omega_d}{\sqrt{1-\zeta^2}}, \tag{A.2}$$

where ω_d is the system's natural undamped oscillatory angular frequency (i.e. angular frequency of the oscillation of the unit step response) of the response, which is:

$$\omega_d = \frac{2\pi}{T}, \tag{A.3}$$

where T is the period of the response oscillation (Fig. 1): $T = t_{p2} - t_{p1}$.

The first peak would occur at latency t_{p1}:

$$t_{p1} = \frac{\pi}{\omega_d}. \tag{A.4}$$

The second peak would occur at latency t_{p2}:

$$t_{p2} = \frac{3\pi}{\omega_d}. \tag{A.5}$$

The relation between the amplitude of the response at the first and second peaks is characterized by the subsidence ratio (R):

$$y(t_{p1}) = Ry(t_{p2}), \tag{A.6}$$

$$R = \frac{y(t_{p1})}{y(t_{p2})}. \tag{A.7}$$

Therefore, R is the amplitude attenuation factor from one cycle to the next in the response (Fig. 1).

Most mathematical development of control theory deals with the design of systems to obtain responses of desired characteristics. Here we have the opposite problem: we are interested in characterizing the system which is responsible for a given response. This can be obtained after a few algebraic manipulations as shown below. R and T characterize the system's response and can be estimated from the response itself according to the formulae shown above and in Fig. 1. To obtain the value of ζ in terms of R, we substitute for $y(t)$ at the first two peaks, after shifting the y-axis zero to 1, and taking natural logarithms:

$$e^{-\zeta\omega_n \frac{\pi}{\omega_d}} = \mathrm{R}e^{-\zeta\omega_n \frac{3\pi}{\omega_d}}, \tag{A.8}$$

$$\log_e e^{-\zeta\omega_n \frac{\pi}{\omega_d}} = \log_e R + \log_e e^{-\zeta\omega_n \frac{3\pi}{\omega_d}}, \tag{A.9}$$

$$-\zeta\omega_n \frac{\pi}{\omega_d} = \log_e R - \zeta\omega_n \frac{3\pi}{\omega_d}, \tag{A.10}$$

$$(-1+3)\zeta\omega_n \frac{\pi}{\omega_d} = \log_e R, \tag{A.11}$$

$$2\pi\zeta \frac{\omega_n}{\omega_d} = \log_e R, \tag{A.12}$$

$$2\pi\zeta \frac{\omega_d}{\omega_d\sqrt{1-\zeta^2}} = \log_e R, \tag{A.13}$$

$$\frac{2\pi\zeta}{\sqrt{1-\zeta^2}} = \log_e R, \tag{A.14}$$

$$\frac{4\pi^2\zeta^2}{1-\zeta^2} = (\log_e R)^2, \tag{A.15}$$

$$4\pi^2\zeta^2 = (\log_e R)^2 - \zeta^2(\log_e R)^2, \tag{A.16}$$

$$\zeta^2(4\pi^2 + (\log_e R)^2) = (\log_e R)^2, \tag{A.17}$$

$$\zeta = \sqrt{\frac{(\log_e R)^2}{4\pi^2 + (\log_e R)^2}}. \tag{A.18}$$

Equation (A.18) provides the value for ζ from R, which can be measured on the recorded systems response (in our case, on the EEG response to SPES). The expected (modeled) system time response, or $y'(t)$, can be calculated from the characteristic equation of the transfer function (A.1) and a standard partial-fraction expansion with its three poles[27] as:

$$y'(t) = 1 - \frac{e^{-\zeta\omega_n t}}{\sqrt{(1-\zeta^2)}} \times [\zeta\sin(\omega_d t) + \sqrt{(1-\zeta^2)}\cos(\omega_d t)]. \tag{A.19}$$

By substituting ζ obtained from Eq. (A.18) into $y'(t)$ in Eq. (A.19) we can calculate the expected (modeled) system's time response ignoring the DC of 1 introduced by the first term on the right of the equation.

A more stable model can in principle be achieved by adding a negative feedback loop (a closed loop system). If $G(s)$ is the transfer function of the open loop system:

$$G(s) = \frac{N(s)}{D(s)} = \frac{\omega_n^2}{s^2 + 2\zeta\omega_n s + \omega_n^2}. \quad \text{(A.20)}$$

Then the transfer function of the closed loop system for a simple proportional controller of K gain is[27]:

$$\frac{O(s)}{I(s)} = \frac{N(s)}{D(s) + KN(s)}. \quad \text{(A.21)}$$

For the second-order closed-loop control system, the transfer function then becomes:

$$\frac{O(s)}{I(s)} = \frac{\omega_n^2}{s^2 + 2\zeta\omega_n s + (K+1)\omega_n^2}. \quad \text{(A.22)}$$

Note that the open loop system is the particular case of the closed loop system where $K = 0$. The closed loop system characteristic equation is:

$$s(s^2 + 2\zeta\omega_n s + (K+1)\omega_n^2) = 0. \quad \text{(A.23)}$$

This system has three poles at $s = 0$ and at:

$$s = -\zeta\omega_n \pm j\omega_n\sqrt{1 + K - \zeta^2}. \quad \text{(A.24)}$$

Following complex number interpretation of the poles, the modulus of s, for s other than 0 is:

$$\sqrt{\zeta^2\omega_n^2 + \omega_n^2(1 + K - \zeta^2)} = \omega_n\sqrt{1+K} \quad \text{(A.25)}$$

and

$$\omega_d = \omega_n\sqrt{(1 + K - \zeta^2)}. \quad \text{(A.26)}$$

Therefore,

$$\cos\theta_1 = \frac{\omega_d}{\text{Modulus of s}} = \frac{\omega_n\sqrt{(1+K-\zeta^2)}}{\omega_n\sqrt{1+K}} = \sqrt{1 - \frac{\zeta^2}{1+K'}}, \quad \text{(A.27)}$$

$$\sin\theta_1 = \frac{\zeta\omega_n}{\omega_n\sqrt{1+K}} = \frac{\zeta}{\sqrt{1+K}}. \quad \text{(A.28)}$$

Following the same arithmetical operations as shown in pages 78 and 79[27] but for the newly defined modulus and ω_d, the time response to a step function of the closed loop second order system, $y'(t)$, is:

$$y'(t) = 1 - \frac{e^{-\zeta\omega_n t}}{\sqrt{(1-\zeta^2)}} \times \left[\frac{\zeta}{\sqrt{1+K}}\sin(\omega_d t) + \sqrt{\frac{1+K-\zeta^2}{1+K}}\cos(\omega_d t)\right], \quad \text{(A.29)}$$

$$y'^{(t)} = 1 - \frac{e^{-\zeta\omega_n t}}{\sqrt{(1-\zeta^2)}\sqrt{1+K}} \times [\zeta\sin(\omega_d t) + \sqrt{1+K-\zeta^2}\cos(\omega_d t)]. \quad \text{(A.30)}$$

The Bode diagram for the closed loop system can be derived as follows:

$$\frac{O(s)}{I(s)} = \frac{\omega_n^2}{s^2 + 2\zeta\omega_n s + (K+1)\omega_n^2}, \quad \text{(A.31)}$$

$$\frac{O(s)}{I(s)} = \frac{1}{\frac{s^2}{\omega_n^2} + \frac{2\zeta\omega_n s}{\omega_n^2} + \frac{(K+1)\omega_n^2}{\omega_n^2}} = \frac{1}{K + 1 - \left(\frac{\omega}{\omega_n}\right)^2 + j2\zeta\left(\frac{\omega}{\omega_n}\right)}. \quad \text{(A.32)}$$

The amplitude at each frequency is represented by the following function which corresponds to the Bode plot representation of amplitude versus frequency:

$$20\log_{10}[\text{Modulus of } O(s)/I(s)] = -20\log_{10}\sqrt{\left[K + 1 - \left(\frac{\omega}{\omega_n}\right)^2\right]^2 + 4\zeta^2\left(\frac{\omega}{\omega_n}\right)^2}. \quad \text{(A.33)}$$

References

1. G. Alarcon, C. N. Guy, C. D. Binnie, S. R. Walker, R. D. Elwes and C. E. Polkey, Intracerebral propagation of interictal activity in partial epilepsy: Implications for source localisation, *J. Neurol. Neurosurg. Psychiatry* **57** (1994) 435–449.
2. G. Alarcon, J. J. Garcia Seoane, C. D. Binnie, M. C. Martin Miguel, J. Juler, C. E. Polkey, R. D. Elwes and J. M. Ortiz Blasco, Origin and propagation of interictal discharges in the acute electrocorticogram. Implications for pathophysiology and surgical treatment of temporal lobe epilepsy, *Brain* **120**(Pt 12) (1997) 2259–2282.
3. C. Martin Miguel Mdel, J. J. Garcia Seoane, A. Valentin, E. Hughes, R. P. Selway, C. E. Polkey

and G. Alarcon, EEG latency analysis for hemispheric lateralisation in Landau-Kleffner syndrome, *Clin. Neurophysiol.* **122** (2011) 244–252.
4. F. Wendling, P. Chauvel, A. Biraben and F. Bartolomei, From intracerebral EEG signals to brain connectivity: Identification of epileptogenic networks in partial epilepsy, *Front. Syst. Neurosci.* **4** (2010) 154.
5. G. Petkov, M. Goodfellow, M. P. Richardson and J. R. Terry, A critical role for network structure in seizure onset: A computational modeling approach, *Front. Neurol.* **5** (2014) 261.
6. M. E. Lacruz, J. J. Garcia Seoane, A. Valentin, R. Selway and G. Alarcon, Frontal and temporal functional connections of the living human brain, *Eur. J. Neurosci.* **26** (2007) 1357–1370.
7. A. Valentin, M. Anderson, G. Alarcon, J. J. G. Seoane, R. Selway, C. D. Binnie and C. E. Polkey, Responses to single pulse electrical stimulation identify epileptogenesis in the human brain *in vivo*, *Brain* **125** (2002) 1709–1718.
8. A. Valentin, G. Alarcon, J. J. Garcia-Seoane, M. E. Lacruz, S. D. Nayak, M. Honavar, R. P. Selway, C. D. Binnie and C. E. Polkey, Single-pulse electrical stimulation identifies epileptogenic frontal cortex in the human brain, *Neurology* **65** (2005) 426–435.
9. D. Flanagan, A. Valentin, J. J. Garcia Seoane, G. Alarcon and S. G. Boyd, Single-pulse electrical stimulation helps to identify epileptogenic cortex in children, *Epilepsia* **50** (2009) 1793–1803.
10. V. Kokkinos, G. Alarcon, R. P. Selway and A. Valentin, Role of single pulse electrical stimulation (SPES) to guide electrode implantation under general anaesthesia in presurgical assessment of epilepsy, *Seizure* **22** (2013) 198–204.
11. R. Matsumoto, D. R. Nair, E. LaPresto, I. Najm, W. Bingaman, H. Shibasaki and H. O. Luders, Functional connectivity in the human language system: A cortico-cortical evoked potential study, *Brain* **127** (2004) 2316–2330.
12. R. Matsumoto, D. R. Nair, A. Ikeda, T. Fumuro, E. Lapresto, N. Mikuni, W. Bingaman, S. Miyamoto, H. Fukuyama, R. Takahashi, I. Najm, H. Shibasaki and H. O. Luders, Parieto-frontal network in humans studied by cortico-cortical evoked potential, *Hum. Brain Mapp.* **33** (2012) 2856–2872.
13. M. Iwasaki, R. Enatsu, R. Matsumoto, E. Novak, B. Thankappen, Z. Piao, T. O'Connor, K. Horning, W. Bingaman and D. Nair, Accentuated cortico-cortical evoked potentials in neocortical epilepsy in areas of ictal onset, *Epileptic Disord.* **12** (2010) 292–302.
14. R. Enatsu, R. Matsumoto, Z. Piao, T. O'Connor, K. Horning, R. C. Burgess, J. Bulacio, W. Bingaman and D. R. Nair, Cortical negative motor network in comparison with sensorimotor network: A cortico-cortical evoked potential study, *Cortex* **49** (2013) 2080–2096.
15. R. Enatsu, Z. Piao, T. O'Connor, K. Horning, J. Mosher, R. Burgess, W. Bingaman and D. Nair, Cortical excitability varies upon ictal onset patterns in neocortical epilepsy: A cortico-cortical evoked potential study, *Clin. Neurophysiol.* **123** (2012) 252–260.
16. C. J. Keller, C. J. Honey, P. Megevand, L. Entz, I. Ulbert and A. D. Mehta, Mapping human brain networks with cortico-cortical evoked potentials, *Philos. Trans. R. Soc. Lond. B Biol. Sci.* **369** (2014) 20130528.
17. K. Terada, N. Usui, S. Umeoka, K. Baba, T. Mihara, K. Matsuda, T. Tottori, T. Agari, F. Nakamura and Y. Inoue, Interhemispheric connection of motor areas in humans, *J. Clin. Neurophysiol.* **25** (2008) 351–356.
18. C. L. Wilson, M. Isokawa, T. L. Babb and P. H. Crandall, Functional connections in the human temporal lobe. I. Analysis of limbic system pathways using neuronal responses evoked by electrical stimulation, *Exp. Brain Res.* **82** (1990) 279–292.
19. D. G. Cherlow, A. M. Dymond, P. H. Crandall, R. D. Walter and E. A. Serafetinides, Evoked response and after-discharge thresholds to electrical stimulation in temporal lobe epileptics, *Arch. Neurol.* **34** (1977) 527–531.
20. A. Rosenblueth, Cortical responses to electric stimulation, *Am. J. Physiol.* **135** (1942) 690–774.
21. R. Matsumoto, D. R. Nair, E. LaPresto, W. Bingaman, H. Shibasaki and H. O. Luders, Functional connectivity in human cortical motor system: A cortico-cortical evoked potential study, *Brain* **130** (2007) 181–197.
22. S. Umeoka, K. Terada, K. Baba, K. Usui, K. Matsuda, T. Tottori, N. Usui, F. Nakamura, Y. Inoue, T. Fujiwara and T. Mihara, Neural connection between bilateral basal temporal regions: Cortico-cortical evoked potential analysis in patients with temporal lobe epilepsy, *Neurosurgery* **64** (2009) 847–855; discussion 855.
23. D. Jimenez-Jimenez, M. Abete-Rivas, D. Martin-Lopez, M. E. Lacruz, R. P. Selway, A. Valentin and G. Alarcon, Incidence of functional bi-temporal connections in the human brain *in vivo* and their relevance to epilepsy surgery, *Cortex* **65** (2015) 208–218.
24. C. Donos, M. D. Maliia, I. Mindruta, I. Popa, M. Ene, B. Balanescu, A. Ciurea and A. Barborica, A connectomics approach combining structural and effective connectivity assessed by intracranial electrical stimulation, *Neuroimage* **132** (2016) 344–358.
25. A. Valentin, G. Alarcon, M. Honavar, J. J. Garcia Seoane, R. P. Selway, C. E. Polkey and C. D. Binnie, Single pulse electrical stimulation for identification of structural abnormalities and prediction of seizure

outcome after epilepsy surgery: A prospective study, *Lancet Neurol.* **4** (2005) 718–726.
26. R. Enatsu, K. Jin, S. Elwan, Y. Kubota, Z. Piao, T. O'Connor, K. Horning, R. C. Burgess, W. Bingaman and D. R. Nair, Correlations between ictal propagation and response to electrical cortical stimulation: A cortico-cortical evoked potential study, *Epilepsy Res.* **101** (2012) 76–87.
27. S. Thompson, *Control Systems. Engineering and Design* (Longman Group UK, United Kingdom).
28. O. D. Creutzfeldt, S. Watanabe and H. D. Lux, Relations between EEG phenomena and potentials of single cortical cells. II. Spontaneous and convulsoid activity, *Electroencephalogr. Clin. Neurophysiol.* **20** (1966) 19–37.
29. C. Donos, I. Mindruta, J. Ciurea, M. D. Maliia and A. Barborica, A comparative study of the effects of pulse parameters for intracranial direct electrical stimulation in epilepsy, *Clin. Neurophysiol.* **127** (2016) 91–101.
30. C. D. Binnie and C. E. Polkey, Surgery for epilepsy, in *Recent Advances in Clinical Neurology* (Churchill Livingstone, London).
31. M. A. Falconer, Genetic and related aetiological factors in temporal lobe epilepsy. A review, *Epilepsia* **12** (1971) 13–31.
32. D. D. Spencer, S. S. Spencer, R. H. Mattson, P. D. Williamson and R. A. Novelly, Access to the posterior medial temporal lobe structures in the surgical treatment of temporal lobe epilepsy, *Neurosurgery* **15** (1984) 667–671.
33. N. Kissani, G. Alarcon, M. Dad, C. D. Binnie and C. E. Polkey, Sensitivity of recordings at sphenoidal electrode site for detecting seizure onset: Evidence from scalp, superficial and deep foramen ovale recordings, *Clin. Neurophysiol.* **112** (2001) 232–240.
34. J. L. Fernandez Torre, G. Alarcon, C. D. Binnie, J. J. Seoane, J. Juler, C. N. Guy and C. E. Polkey, Generation of scalp discharges in temporal lobe epilepsy as suggested by intraoperative electrocorticographic recordings, *J. Neurol. Neurosurg. Psychiatry* **67** (1999) 51–58.
35. N. Akanuma, G. Alarcon, F. Lum, N. Kissani, M. Koutroumanidis, N. Adachi, C. D. Binnie, C. E. Polkey and R. G. Morris, Lateralising value of neuropsychological protocols for presurgical assessment of temporal lobe epilepsy, *Epilepsia* **44** (2003) 408–418.
36. A. Kumar, A. Valentin, D. Humayon, A. L. Longbottom, D. Jimenez-Jimenez, N. Mullatti, R. C. D. Elwes, I. Bodi, M. Honavar, J. Jarosz, R. P. Selway, C. E. Polkey, I. Malik and G. Alarcon, Preoperative estimation of seizure control after resective surgery for the treatment of epilepsy, *Seizure-Eur. J. Epilepsy* **22** (2013) 818–826.
37. I. Nauhaus, L. Busse, M. Carandini and D. L. Ringach, Stimulus contrast modulates functional connectivity in visual cortex, *Nat. Neurosci.* **12** (2009) 70–76.
38. J. D. Cowan, J. Neuman and W. van Drongelen, Wilson-Cowan equations for neocortical dynamics, *J. Math. Neurosci.* **6** (2016) 1.
39. O. D. Creutzfeldt, S. Watanabe and H. D. Lux, Relations between EEG phenomena and potentials of single cortical cells. I. Evoked responses after thalamic and epicortical stimulation, *Electroencephalogr. Clin. Neurophysiol.* **20** (1966) 1–18.
40. D. S. Barth and W. Sutherling, Current source-density and neuromagnetic analysis of the direct cortical response in rat cortex, *Brain Res.* **450** (1988) 280–294.
41. G. Alarcon, J. Martinez, S. V. Kerai, M. E. Lacruz, R. Q. Quiroga, R. P. Selway, M. P. Richardson, J. J. Garcia Seoane and A. Valentin, *In vivo* neuronal firing patterns during human epileptiform discharges replicated by electrical stimulation, *Clin. Neurophysiol.* **123** (2012) 1736–1744.
42. D. Nayak, A. Valentin, R. P. Selway and G. Alarcon, Can single pulse electrical stimulation provoke responses similar to spontaneous interictal epileptiform discharges? *Clin. Neurophysiol.* **125** (2014) 1306–1311.
43. Z. Voysey, D. Martin-Lopez, D. Jimenez-Jimenez, R. P. Selway, G. Alarcon and A. Valentin, Electrical stimulation of the anterior cingulate gyrus induces responses similar to K-complexes in awake humans, *Brain Stimul.* **8** (2015) 881–890.